$p_{z_n} \equiv 0$ holding in a finite interval inside $[\tau_1, \tau_2]$. It follows that no finite singular arcs exist for the optimal throttle setting in $[\tau_1, \tau_2]$.

One special case of the engine model (9) is a nonlinear first-order lag

$$\eta' = -a(\eta)(\eta - \eta_{\text{com}}) \tag{32}$$

where the time-constant $1/a$ depends on the current engine power level specified by η. The engine model for an F-16 aircraft in Ref. 3, for instance, has this feature. Also, a linear nth-order model

$$\eta^{(n)} + a_{n-1}\eta^{(n-1)} + \cdots + a_1\eta' + a_0\eta = a_0\eta_{\text{com}} \tag{33}$$

is certainly another special case of Eq. (9), where the a_i coefficients are positive constants such that the polynomial $p(s) = s^n + a_{n-1}s^{n-1} + \cdots + a_0$ is Hurwitz. [It may be further necessary that $p(s) = 0$ have only negative real roots for Eq. (33) to be a reasonable model, since by definition $0 \le \eta \le 1$, and no overshoot in η from Eq. (33) should exist for $\eta_{\text{com}} = 1.0$ or $\eta_{\text{com}} = 0$.]

When the weighting ϕ is set to zero in the performance index (15), i.e., the reduction of time-of-flight is not a part of the optimization objective, Eq. (28) can be satisfied when $L(h, X) = h - F(X) = 0$. In other words, singular optimal η_{com} can occur only when $\phi = 0$ and the terrain is perfectly followed. A similar conclusion is obtained and a numerical example is given in Ref. 1 for no engine dynamics.

The conclusion in Proposition 1 can be further generalized to include the case where the engine dynamic characteristics are also dependent on Mach number and altitude. Suppose that the engine dynamics are modeled by

$$\eta^{(n)} = a\left(\eta, \ldots, \eta^{(n-1)}, V, h\right) + b\left(\eta, \ldots, \eta^{(n-1)}, V, h\right)\eta_{\text{com}} \tag{34}$$

Then we have the following result.

Proposition 2. Assume all of the conditions stated in Proposition 1, except that now the engine model is also dependent on Mach number and altitude as defined by Eq. (34), and $b(\eta, \ldots, \eta^{(n-1)}, V, h) \neq 0$ along the optimal trajectory. Then, the optimal throttle setting $\eta^*_{\text{com}}(\tau)$ must be of bang-bang type in any finite interval in $[0, \tau_f]$ where the optimal $\alpha^*(\tau)$ is interior.

Proof. In this case the only change in the optimality conditions used in the proof of Proposition 1 is in the p_V equation,

$$\begin{aligned} p'_V = -\frac{\partial H}{\partial V} &= -p_h \sin\gamma - p_X \cos\gamma \\ &- p_V\left(z_1 \cos\alpha \frac{\partial A_{T\max}}{\partial V} - \frac{\partial A_D}{\partial V}\right) \\ &+ \frac{p_\gamma}{V}\left[\frac{1}{V}(A_{T\max} z_1 \sin\alpha + A_L) - z_1 \sin\alpha \frac{\partial A_{T\max}}{\partial V} - \frac{\partial A_L}{\partial V}\right. \\ &\left. - \frac{\cos\gamma}{V}\right] - p_{z_n}\left(\frac{\partial a(z, V, h)}{\partial V} + \frac{\partial b(z, V, h)}{\partial V}\eta_{\text{com}}\right) \end{aligned} \tag{35}$$

where z is the same as defined before. But upon assuming a singular arc for η^*_{com}, then $p_{z_n} \equiv 0$ and the last term in Eq. (35) drops out. Thus, Eqs. (18) and (35) are identical in this interval. The rest of the proof based on contradiction then follows exactly the proof of Proposition 1.

When the aircraft is in high angle-of-attack flight, the engine characteristics may also be dependent on α. Following a similar proof, we have the following.

Proposition 3 Now assume that $T_{\max}$ is a C^1 function of Mach number, represented by V, altitude h, and angle of attack α, and the engine dynamics are also α dependent,

$$\eta^{(n)} = a\left(\eta, \ldots, \eta^{(n-1)}, V, h, \alpha\right) + b\left(\eta, \ldots, \eta^{(n-1)}, V, h, \alpha\right)\eta_{\text{com}} \tag{36}$$

If all of the conditions in Proposition 1 hold and $b(\eta, \ldots, \eta^{(n-1)}, V, h, \alpha) \neq 0$ along the optimal trajectory, then the optimal throttle setting $\eta^*_{\text{com}}(\tau)$ must be of bang-bang type in any finite interval in $[0, \tau_f]$ where the optimal $\alpha^*(\tau)$ is interior.

The main difference in the proof in this case is that the optimality condition $\partial H/\partial\alpha = 0$ will have an extra term involving $\partial A_{T_{\max}}/\partial\alpha$ in each of the parentheses following p_V and p_γ as compared to Eq. (22), and two extra terms involving $p_{z_n}\partial a/\partial\alpha$ and $p_{z_n}\partial b/\partial\alpha$. But these terms either become zero because of condition (24), or cancel each other when setting the determinant of the algebraic system in p_V and p_γ to zero. Eventually, a condition exactly the same as Eq. (29) is arrived at that again eliminates the possibility of singular throttle control. The detailed proof is omitted because of space limitations.

As a concluding remark, it should be stressed that although the preceding analysis reveals that bang-bang throttle control is a general property of the optimal terrain-following problem, which requires little specifics on the engine model, the number of throttle setting switchings is expected to depend strongly on the particular engine model assumed.

IV. Conclusions

This Note shows that for a class of nonlinear engine dynamic models of arbitrary order that can also be Mach, altitude, and angle-of-attack dependent, the optimal throttle setting for aircraft terrain-following flight in most cases is of bang-bang type whenever the optimal angle of attack is interior. The only case where a singular throttle control may appear is when the time-of-flight is not included in the performance index and the terrain is followed exactly. The same behavior of the optimal throttle setting is obtained in Ref. 1 where no engine dynamics are included. This result suggests that the usual practice of ignoring engine dynamics in aircraft trajectory optimization work does not lead to incorrect conclusions. Because of the space limitation, the effects of engine dynamics on optimal aircraft terrain-following performance are not explored numerically in this Note, but will be investigated in our future studies.

References

[1]Lu, P., and Pierson, B. L., "Optimal Aircraft Terrain-Following Analysis and Trajectory Generation," *Journal of Guidance, Control, and Dynamics*, Vol. 18, No. 3, 1995, pp. 555–560.

[2]Bryson, A. E., and Ho, Y. C., *Applied Optimal Control*, Hemisphere, New York, 1975, Chap. 2.

[3]Stevens, B. L., and Lewis, F. L., *Aircraft Control and Simulation*, Wiley, New York, 1992, Chap. 3, p. 127.

Long Flight-Time Range-Optimal Aircraft Trajectories

Hans Seywald*
Analytical Mechanics Associates, Inc., Hampton, Virginia 23666

Introduction

In Ref. 1, indirect solutions based on Pontryagin's minimum principle[2] were obtained for the problem of maximizing the downrange of a high-performance atmospheric flight vehicle operating in the vertical plane. The present Note is based on an identical aircraft model and extends the results obtained in Ref. 1.

Control variables are the load factor that appears nonlinearly in the equations of motion and the throttle setting that appears only linearly. Both controls are subject to fixed bounds. Additionally, a dynamic pressure limit is imposed, which represents a first-order state-inequality constraint.[2]

Received Aug. 13, 1994; revision received April 20, 1995; accepted for publication June 27, 1995;

*Supervising Engineer, 17 Research Drive, working under contract at Guidance and Controls Branch, NASA Langley Research Center, Hampton, VA 23681. Member AIAA.

In Ref. 1, the flight time was kept fixed at 60 s, and the effect of the prescribed load factor limit on the optimal switching structure was investigated. For prescribed flight times greater than 62 s, the optimal solution could not be found. The present Note fills this gap, and the optimal solution is presented for prescribed flight times between 70 and 120 s. All trajectories obtained here and in Ref. 1 involve singular control[2] along arcs with active dynamic pressure limit.

Aircraft Model

Because of nonconvexities in the hodograph associated with the original aircraft model it is necessary to convexize the equations of motion[3] before certain singular control cases can be analyzed. For details the reader is referred to Ref. 1. Because of some typographical errors in Ref. 1 (the author is indebted to Anil V. Rao for identifying these errors) the convexized model is completely restated here. The equations of motion are

$$\dot{E} = [\delta(T - D + D_{\max}) - D_{\max}](v/mg) \tag{1}$$

$$\dot{h} = v \sin\gamma \tag{2}$$

$$\dot{\gamma} = (g/v)[(L/mg) - \cos\gamma] \tag{3}$$

$$\dot{x} = v \cos\gamma \tag{4}$$

The specific energy E replacing velocity v, the altitude h, the flight-path angle γ, and the range x are the state variables. Load factor n and the power setting δ are the control variables. The mass m (in kilograms) of the vehicle and the gravitational acceleration g (in meters per second squared) are assumed to be constant, namely,

$$m = 37{,}000/2.2, \qquad g = 9.80665$$

Velocity v is a short notation for $v = \sqrt{[2g(E-h)]}$. The air density ρ in kilograms per cubic meter is given by

$$\rho(h) = 1.225\, e^{y}$$

with

$$y = -0.12122693\,\bar{h} + r - 1.0228055, \qquad r = 1.0228055\, e^{-z}$$

$$z = -3.48643241\,10^{-2}\bar{h} + 3.50991865\,10^{-3}\bar{h}^2$$

$$- 8.33000535\,10^{-5}\bar{h}^3 + 1.15219733\,10^{-6}\bar{h}^4$$

Here and in the following, h and $\bar{h}$ denote altitude in meters and kilometers, respectively. The temperature θ in Kelvin and the speed of sound a in meters per second are given by

$$\theta(h) = 292.1 - 8.87743\,\bar{h} + 0.193315\,\bar{h}^2 + 3.72\,10^{-3}\bar{h}^3$$

$$a(h) = 20.0468\sqrt{\theta}$$

The Mach number is given by $M = v/a(h)$, and the cross-section area S in square meters has the value $S = 60$. The lift L, the drag D, the maximum drag $D_{\max}$, and the maximum thrust T in newtons are given as functions of h, M, and n, respectively, namely,

$$q = \tfrac{1}{2}\rho(h)v^2 S, \qquad L = mgn$$

$$D = q\left[C_{D0}(M) + K(M)\,(m^2g^2/q^2)n^2\right], \qquad D_{\max} = D|_{n=n_{\max}}$$

$$C_{D0} = \frac{\sum_{i=0}^{4} a_i \cdot M^i}{\sum_{i=0}^{4} b_i \cdot M^i} \qquad K = \frac{\sum_{i=0}^{4} c_i \cdot M^i}{\sum_{i=0}^{5} d_i \cdot M^i}$$

$$T(h, M) = \left(\sum_{i=0}^{5} e_i(M) \cdot \bar{h}^i\right) \cdot \frac{9.80665}{2.2}$$

with

$$e_i(M) = \sum_{j=0}^{5} f_{ij} \cdot M^j, \qquad i = 0, 1, \ldots, 5$$

The numerical values of the constants a_i, b_i, c_i, d_i, and f_{ij} can be found in Table 1 and represent a high-performance fighter interceptor. The factor 9.80665/2.2 in the thrust equation stems from the conversion from pounds force to newtons.

Problem Formulation

Loosely speaking, the problem considered in this Note can be stated as follows: find the control functions of time $\delta(t)$ and $n(t)$ such that the downrange x is maximized subject to certain boundary conditions, control constraints, and state constraints. Explicitly, in Mayer form the problem is given by

$$\min\, -x(t_f) \tag{5}$$

subject to the state equations (1–4), the control constraints

$$-n_{\max} \le n \le +n_{\max}, \qquad 0 \le \delta \le 1 \tag{6}$$

the state constraint

$$v - v_{\max}(h) \le 0 \tag{7}$$

where $v_{\max}(h)$ is chosen such that Eq. (7) represents a dynamic pressure limit, and the boundary conditions where specific energy, altitudes, and range are in meters and flight-path angle is in radians:

$$E(0) = 38029.207 \tag{8a}$$

$$h(0) = 12119.324 \tag{8b}$$

$$\gamma(0) = 0 \tag{8c}$$

$$x(0) = 0 \tag{8d}$$

$$E(t_f) = 9000 \tag{8e}$$

$$h(t_f) = 942.292 \tag{8f}$$

$$\gamma(t_f) = -0.2 \tag{8g}$$

In Ref. 1 it was observed that a change in the optimal switching structure occurs if the prescribed flight time is increased to values $\ge$63 s. For these flight times the correct switching structure could not be found. The present Note fills this gap by presenting the optimal solution (in second) for long fight times, e.g.,

$$t_f = 120 \tag{9}$$

The value of the load factor limit is kept at $n_{\max} = 10$.

Optimal Switching Structure

With $n_{\max} = 10$, and with a prescribed flight time t_f greater than 62.053 s, the optimal solution consists of six arcs. (Trajectories with a prescribed flight time greater than 120 s have not been attempted.) The controls n and δ and the multiplier μ associated with the dynamic pressure limit (7) are as follows.

Arc 1: the dynamic pressure limit (7) is not active; the throttle δ is riding its upper bound; the load factor is determined from $\partial H/\partial n = 0$:

$$n = \frac{\lambda_\gamma}{\lambda_E}\frac{g\,q}{2\,v^2 mgK}, \qquad \delta = 1, \qquad \mu = 0$$

Arc 2: the dynamic pressure limit (7) is active; the load factor n is as large as possible; the throttle δ is determined implicitly through Eq. (7). Here and along arc 3, the upper bound on the absolute value of the load factor is implicitly determined through the condition that the throttle required to stay on the constraint (7) must be less or equal 1,

$$n = \frac{q}{mg}\sqrt{\frac{T - (vmg/g)\sin\gamma[v'_{\max} + (q/v)] - qC_{D0}}{qK}}$$

$$\delta = 1, \qquad \mu = \frac{\lambda_\gamma}{n}\frac{q}{2\,K\,vmg} - \lambda_E\frac{v}{g}$$

Table 1 Coefficients for thrust and drag model

	$i=0$	$i=1$	$i=2$	$i=3$	$i=4$	$i=5$
a_i	$+2.61059846050\ 10^{-2}$	$-8.57043966269\ 10^{-2}$	$+1.07863115049\ 10^{-1}$	$-6.44772018636\ 10^{-2}$	$+1.64933626507\ 10^{-2}$	—
b_i	$+1.37368651246\ 10^{0}$	$-4.57116286752\ 10^{0}$	$+5.72789877344\ 10^{0}$	$-3.25219000620\ 10^{0}$	$+7.29821847445\ 10^{-1}$	—
c_i	$+1.23001735612\ 10^{0}$	$-2.97244144190\ 10^{0}$	$+2.78009092756\ 10^{0}$	$-1.16227834301\ 10^{0}$	$+1.81868987624\ 10^{-1}$	—
d_i	$+1.42392902737\ 10^{+1}$	$-3.24759126471\ 10^{+1}$	$+2.96838743792\ 10^{+1}$	$-1.33316812491\ 10^{+1}$	$+2.87165882405\ 10^{0}$	$-2.27239723756\ 10^{-1}$
f_{i0}	$+0.11969995703\ 10^{6}$	$-0.14644656421\ 10^{5}$	$-0.45534597613\ 10^{3}$	$+0.49544694509\ 10^{3}$	$-0.46253181596\ 10^{2}$	$+0.12000480258\ 10^{1}$
f_{i1}	$-0.35217318620\ 10^{6}$	$+0.51808811078\ 10^{5}$	$+0.23143969006\ 10^{4}$	$-0.22482310455\ 10^{4}$	$+0.20894683419\ 10^{3}$	$-0.53807416658\ 10^{1}$
f_{i2}	$+0.60452159152\ 10^{6}$	$-0.95597112936\ 10^{5}$	$-0.38860323817\ 10^{4}$	$+0.39771922607\ 10^{4}$	$-0.36835984294\ 10^{3}$	$+0.94529288471\ 10^{1}$
f_{i3}	$-0.43042985701\ 10^{6}$	$+0.83271826575\ 10^{5}$	$+0.12357128390\ 10^{4}$	$-0.30734191752\ 10^{4}$	$+0.29388870979\ 10^{3}$	$-0.76204728620\ 10^{1}$
f_{i4}	$+0.13656937908\ 10^{6}$	$-0.32867923740\ 10^{5}$	$+0.55572727442\ 10^{3}$	$+0.10635494768\ 10^{4}$	$-0.10784916936\ 10^{3}$	$+0.28552696781\ 10^{1}$
f_{i5}	$-0.16647992124\ 10^{5}$	$+0.49102536402\ 10^{4}$	$-0.23591380327\ 10^{3}$	$-0.13626703723\ 10^{3}$	$+0.14880019422\ 10^{2}$	$-0.40379767869\ 10^{0}$

Table 2 Lengths of subarcs in seconds for trajectories with prescribed flight times between 62.053 and 120 s

t_f	Δt_1	Δt_2	Δt_3	Δt_4	Δt_5	Δt_6
62.053	28.719	0.559	0	29.370	2.307	1.098
70	36.077	0.849	0.443	29.239	2.294	1.098
95	60.166	1.669	0.575	29.215	2.276	1.098
120	85.071	1.763	0.576	29.218	2.274	1.098

Arc 3: the dynamic pressure limit (7) is active; the load factor n is as small (in the sense of as large negative) as possible; the throttle δ is determined implicitly through Eq. (7),

$$n = -\frac{q}{mg}\sqrt{\frac{T-(vmg/g)\sin\gamma[v'_{\max}+(q/v)]-qC_{D0}}{qK}}$$

$$\delta = 1, \qquad \mu = \frac{\lambda_\gamma}{n}\frac{q}{2Kvmg} - \lambda_E\frac{v}{g}$$

Arc 4: the dynamic pressure limit (7) is active; the load factor n is singular; the throttle δ is determined implicitly through Eq. (7),

$$n = \left[1 - \frac{v'_{\max}v}{g}\right]\cos\gamma$$

$$\delta = \frac{D_{\max}+(vmg/g)\sin\gamma[v'_{\max}+(g/v)]}{T - D|_{n\text{ as above}} + D_{\max}}$$

$$\mu = -\lambda_E(v/g)$$

This control logic represents a first-order singular control case. At the beginning of this arc the following two additional conditions have to be satisfied:

$$\lambda_\gamma = 0, \qquad \lambda_h - \lambda_x\tan\gamma + \lambda_E\left[1 + \frac{v'_{\max}v}{g}\right] = 0$$

Arc 5: the dynamic pressure limit (7) is active; the load factor n is riding its upper bound $n_{\max}$; the throttle δ is determined implicitly through Eq. (7),

$$n = n_{\max}, \qquad \delta = \frac{D_{\max}+(vmg/g)\sin\gamma[v'_{\max}+(g/v)]}{T - D|_{n\text{ as above}} + D_{\max}}$$

$$\mu = -\lambda_E(v/g)$$

Arc 6: the dynamic pressure limit (7) is not active; the load factor n is riding its upper bound $n_{\max}$; the throttle δ is riding its lower bound, 0,

$$n = n_{\max}, \qquad \delta = 0, \qquad \mu = 0$$

It is interesting to note that this switching structure becomes identical to the one obtained in Ref. 1 if arc 3 is deleted.

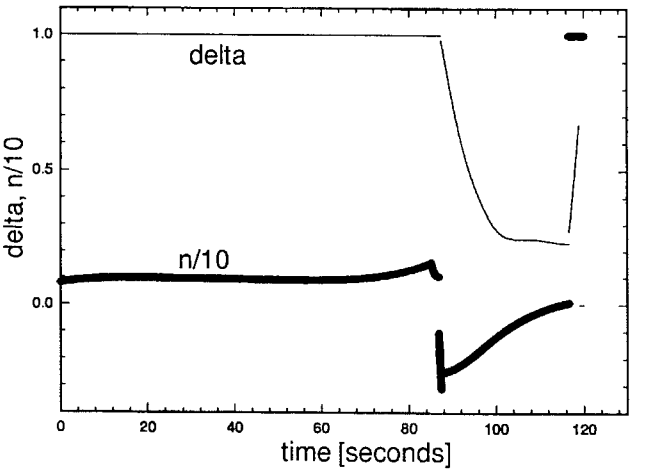

Fig. 1 Time histories of controls and δ and $n/10$ for t_f = 120 s.

Numerical Results

Figure 1 shows the time histories of throttle δ and load factor n for a prescribed flight time of 120 s. In Table 2, the lengths of individual subarcs are listed for solutions obtained with various prescribed flight times. Note that arc 3 vanishes as t_f approaches 62.053 s. In the limiting case, the switching structure found here reduces to the one found in Ref. 1.

Summary

Long flight-time, range-optimal trajectories are synthesized for a high-performance atmospheric flight vehicle operating in the vertical plane. The trajectories are subject to a dynamic pressure limit and a load factor limit. In the context of optimal control these represent a first-order state inequality constraint and a control constraint, respectively. Numerical solutions generated for flight times between 62.053 and 120 s consist of six arcs, along four of which the dynamic pressure limit is active. Singular control along the active state constraint represents a significant part of the trajectory. For shorter flight times the optimal solution was presented in an earlier paper.

Acknowledgments

This work was supported by NASA Langley Research Center under Contract NAS1-18935. Helpful comments and suggestions concerning the aircraft modeling were provided by Anil V. Rao.

References

[1]Seywald, H., Cliff, E. M., and Well, K. H., "Range Optimal Trajectories for an Aircraft Flying in the Vertical Plane," *Journal of Guidance, Control, and Dynamics*, Vol. 17, No. 2, 1994, pp. 389–398.

[2]Bryson, A. E., and Ho, Y. C., *Applied Optimal Control*, Hemisphere, New York, 1975.

[3]Cliff, E. M., Seywald, H., and Bless, R. R., "Hodograph Analysis in Aircraft Trajectory Optimization," *Proceedings of the AIAA Guidance, Navigation, and Control Conference* (Monterey, CA), AIAA, Washington, DC, 1993, pp. 363–371 (AIAA Paper 93-3742).